

Many-body protected entanglement generation in interacting spin systems

A. M. Rey,¹ L. Jiang,² M. Fleischhauer,³ E. Demler,² and M. D. Lukin^{1,2}

¹*Institute for Theoretical Atomic, Molecular and Optical Physics, Cambridge, Massachusetts 02138, USA*

²*Physics Department, Harvard University, Cambridge, Massachusetts 02138, USA*

³*Fachbereich Physik, Technische Universitat Kaiserslautern, D-67663 Kaiserslautern, Germany*

(Received 4 January 2008; revised manuscript received 23 March 2008; published 5 May 2008)

We discuss a method to achieve decoherence resistant entanglement generation in strongly interacting ensembles of two-level spin systems. Our method uses designed gapped Hamiltonians to create a protected manifold of multidegenerate levels which is robust against local decoherence processes. We apply the protected evolution to achieve decoherence resistant generation of many-particle Greenberger-Horne-Zeilinger (GHZ) states in two specific physical systems, trapped ions and neutral atoms in optical lattices, and discuss how to engineer the desired many-body protected manifold with them. We analyze the fidelity of GHZ generation and show our method can significantly increase the sensitivity in frequency spectroscopy.

DOI: [10.1103/PhysRevA.77.052305](https://doi.org/10.1103/PhysRevA.77.052305)

PACS number(s): 03.67.Mn, 03.75.Gg, 03.75.Mn, 06.20.-f

I. INTRODUCTION

Entangled states are a fundamental resource in quantum information and quantum communication science [1,2]. Additionally, certain entangled atomic states (also known as spin squeezed states) in principle allow to significantly improve the resolution in Ramsey spectroscopy [3,4]. However, in practice entangled states are difficult to prepare and maintain, and noise and decoherence rapidly collapses them into classical statistical mixtures. Thus, one of the most important challenges in modern quantum physics is the design of robust and most importantly decoherence resistant methods for entanglement generation.

We have recently proposed a method [5] that allows for noise resistant generation of entangled states. Our method uses designed gapped Hamiltonians to create a protected manifold of degenerate levels which is robust against local decoherence processes. While the large number of degrees of freedom in the manifold allows us to create various quantum superpositions and to exploit rich dynamical evolution (suitable, for example, for precision spectroscopy), the energy gap prevents decoherence as local excitations become energetically suppressed. A simple example of a many-body spin Hamiltonian that illustrates the idea of our scheme is a multispin system with isotropic ferromagnetic interactions. These interactions will naturally align the spins. While all of the spins can be rotated together around an arbitrary axis without cost of energy, local spin flips are energetically forbidden.

This paper presents a detailed analysis of this method when used in trapped ions and cold atoms in optical lattices. We demonstrate its applicability for decoherence resistant generation of N -particle Greenberger-Horne-Zeilinger (GHZ) states [6] and the potential of the latter to be used for Heisenberg-limited spectroscopy. The paper is organized as follows: In Sec. II we review one of the standard procedures used to generate multiparticle GHZ entangled states and show the detrimental effect of phase decoherence in this scheme. In Sec. III we explain the idea of a many-body protected manifold (MPM) and discuss how and under what conditions it can significantly reduce the effects of decoherence.

In Sec. IV we discuss ways to implement the protected manifold in trapped ion systems and the applicability of the gap protected evolution to significantly improve the phase sensitivity in precision spectroscopy. In this section we also analyze the fidelity of the GHZ generation, taking into account nonideal conditions. In Sec. V we study how to engineer the long-range Hamiltonian required for the gap protected evolution in optical lattice systems interacting via short-range interactions and discuss the effectiveness of the MPM for GHZ generation. In Sec. VI we analyze in such systems the effect of nonideal conditions such as the magnetic trapping confinement and finally conclude in Sec. VII.

II. SPIN SQUEEZING IN INTERACTING SPIN ENSEMBLES

A. Ideal case

In this section we start by reviewing a method to generate multiparticle entangled states in a system of N spinor atoms with two relevant internal states which we identify with the effective spin index $\sigma = \uparrow, \downarrow$. The basic idea is to evolve an initially uncorrelated state with the so-called squeezing Hamiltonian,

$$\hat{H}_z = \chi \hat{J}_z^{(0)2}. \quad (1)$$

As shown in Refs. [7,8] the \hat{H}_z Hamiltonian can be implemented in trapped ions by using the collective vibrational motion of the ions in a linear trap driven by illuminating them with a laser field [3,4,9]. In Eq. (1) we used $\hat{J}_\alpha^{(0)}$ to denote the collective spin operators of the N atoms: $\hat{J}_\alpha^{(0)} = \frac{1}{2} \sum_i \hat{\sigma}_i^\alpha$, where $\alpha = x, y, z$ and $\hat{\sigma}_i^\alpha$ is a Pauli operator acting on the i th atom. In this paper we will use units such that $\hbar = 1$ and assume N to be even.

To describe the entanglement generation process we use the basis spanned by collective pseudospin states denoted as $|J, M, \beta\rangle_z$ [10]. These states satisfy the eigenvalue relations $\hat{J}^{(0)2}|J, M, \beta\rangle_z = J(J+1)|J, M, \beta\rangle_z$ and $\hat{J}_z^{(0)}|J, M, \beta\rangle_z = M|J, M, \beta\rangle_z$, with $J = N/2, \dots, 0$ and $-J \leq M \leq J$. β is an additional quantum number associated with the permutation

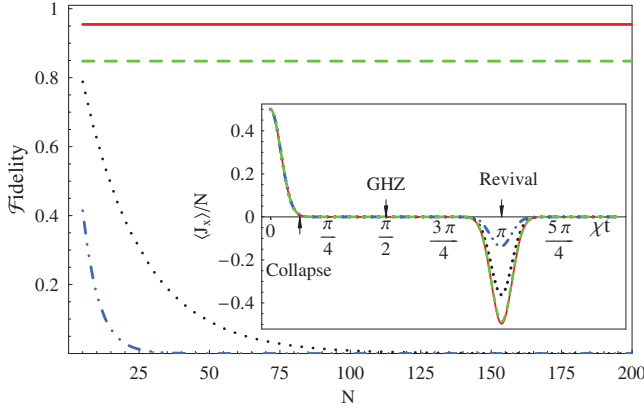


FIG. 1. (Color online) Fidelity of GHZ generation vs N with and without gap protection. We assume a noise with steplike spectral density with amplitude $f=2$ kHz and cutoff frequency $\omega_c=6$ kHz. The solid red and dashed green lines are for a protected system, $\lambda=\chi$, with $\chi=25$ and 10 kHz, respectively. The black dotted and blue dotted-dashed lines are for an unprotected system, $\lambda=0$, with the same parameters $\chi=25$ and 10 kHz, respectively. In the inset we show $\langle \hat{J}_x^{(0)}(t) \rangle / N$ for $N=50$ and the various curves are for the same parameters as those shown in the main plot. The horizontal axis in the inset is in units of \hbar .

group which is required to form a complete set of labels for all the 2^N possible states. The process starts by preparing the system at $t=0$ in a fully polarized state along the x direction $|N/2, N/2\rangle_x$ (as any state with $J=N/2$ is uniquely characterized by M , for denoting them we omit the additional β label). Fully polarized states along x can be written as a superposition of states with different M values along the z direction, $\sum_M C_M |N/2, M\rangle_z$. During the evolution the Hamiltonian imprints an M^2 -dependent phase to the different components. At first the winding of the phases leads to a collapse of $\langle \hat{J}_x^{(0)} \rangle$. However, at time $\chi t_{\text{rev}} = \pi$ all components rephase with opposite polarization, and a perfect revival of the initial state is observed with $\langle \hat{J}_x^{(0)} \rangle = -N/2$ (see Fig. 1). Specifically, the time evolution of $\langle \hat{J}_x^{(0)} \rangle$ for systems with $N \gg 1$ can be shown to be given by

$$\langle \hat{J}_x^{(0)} \rangle = \frac{N}{2} \sum_{k=0,1,2,\dots} (-1)^k e^{-N/2(\chi t - k\pi)^2}. \quad (2)$$

Right at time $t_0 = t_{\text{rev}}/2$ the system becomes a macroscopic superposition of fully polarized states along the $\pm x$ direction, i.e., a N -particle GHZ state of the form

$$|\psi_x^{\text{GHZ}}\rangle \equiv \frac{1}{\sqrt{2}} \left(e^{-i\phi_+} \left| \frac{N}{2}, \frac{N}{2} \right\rangle_x + e^{i\phi_-} \left| \frac{N}{2}, -\frac{N}{2} \right\rangle_x \right), \quad (3)$$

with ϕ_{\pm} real phases given by $-\pi/4$ and $\pi/4 + N\pi/2$.

Recent experiments [3,4] have used this type of scheme to generate GHZ states in trapped ions with the aim to perform precision measurements of ω_0 , the energy splitting between \uparrow and \downarrow levels. Ideally the use of GHZ states should enhance the phase sensitivity to the fundamental Heisenberg limit [11]. However, decoherence significantly limited the applicability of the method.

B. Effect of decoherence

To understand the detrimental effect of decoherence we first assume that the dominant type of decoherence is single-particle dephasing. Such dephasing comes from processes that, while preserving the populations in the atomic levels, randomly change the phases leading to a decay of the off-diagonal density matrix elements. We model the phase decoherence by adding to Eq. (1) the following Hamiltonian [12]:

$$\hat{H}_{\text{env}} = \frac{1}{2} \sum_i h_i(t) \hat{\sigma}_i^z, \quad (4)$$

where $h_i(t)$ are assumed to be independent stochastic Gaussian processes with zero mean and with autocorrelation function $\overline{h_i(t)h_j(\tau)} = \delta_{ij}f(t-\tau)$. Here the overbar denotes averaging over the different random outcomes. In what follows we will use the property that zero mean Gaussian variables satisfy $\exp[-i\int_0^t d\tau h(\tau)] = \exp[-\Gamma(t)]$, with $\Gamma(t) = \frac{1}{2} \int_0^t dt_1 \int_0^t dt_2 f(t_1 - t_2)$ [13].

Phase decoherence causes an exponential decay of the revival peak and N -dependent decay of the fidelity, defined as $\mathcal{F}(t_0) = \langle \psi_x^{\text{GHZ}} | \hat{\rho}(t_0) | \psi_x^{\text{GHZ}} \rangle$ (see Fig. 1). Qualitatively the effect of phase decoherence on the evolving state can be understood from the energy levels of \hat{H}_z (see Fig. 2). \hat{H}_z

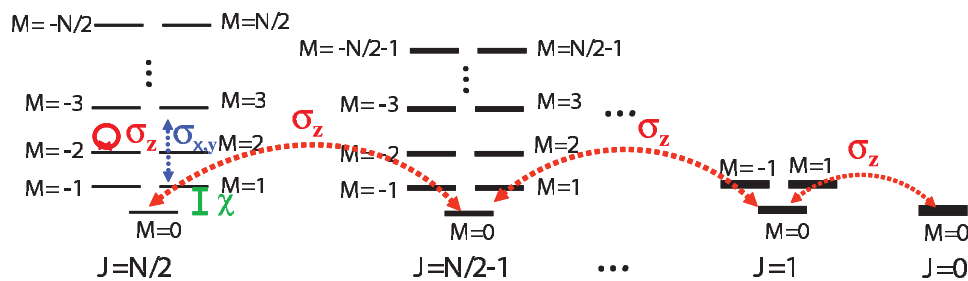


FIG. 2. (Color online) Schematic representation of the energy levels of the $\chi \hat{J}_z^{(0)2}$ Hamiltonian and the effect of the different types of noise. As states with different J but equal $|M|$ are degenerate, in the presence of phase decoherence (σ_z noise) they are populated during the time evolution. $\sigma_{x,y}$ noises couple states which differ by ± 1 units of M and therefore the small energy gap between them, of the order of χ , naturally protects the system from these type of processes.

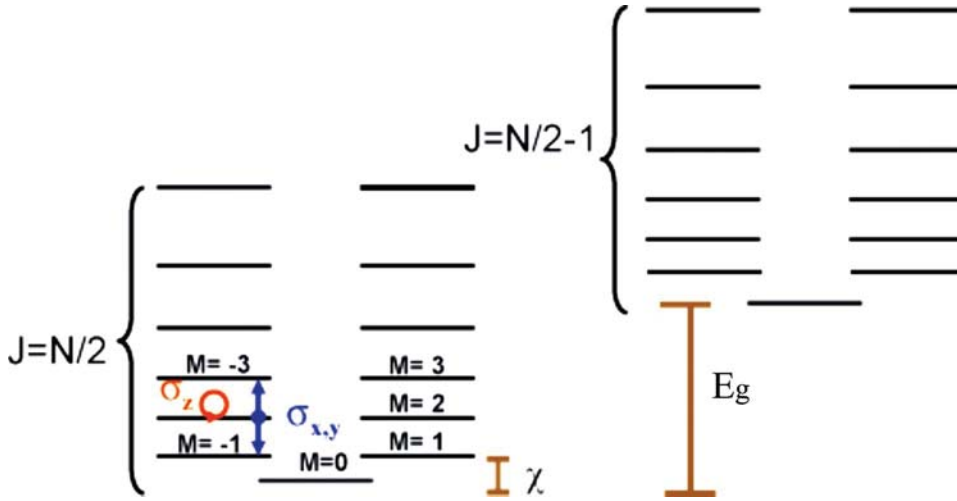


FIG. 3. (Color online) Schematic representation of the energy levels of the \hat{H}_c Hamiltonian. \hat{H}_{prot} lifts the degeneracy of the different J manifolds and suppresses (in the slow noise limit) couplings between them. So if a $t=0$ system is in the MPM it remains there.

commutes with both $\hat{J}_z^{(0)}$ and $\hat{J}^{(0)2}$, however, \hat{H}_{env} only commutes with $\hat{J}_z^{(0)}$. Consequently, in the presence of phase decoherence transitions between different J subspaces are allowed as long as M is conserved. As all the states with the same $|M|$ value are degenerate, there is no energy barrier to prevent such transitions and very quickly the initially populated $J=N/2$ manifold is depleted and the fidelity of generating the GHZ state significantly degraded. Moreover, the degradation scales exponential with increasing N due to the exponential scalability of the number of accessible states to which the initial $J=N/2$ population can be transferred to. Maximally polarized states $|J=N/2, \pm N/2\rangle$ do not couple to other J manifolds, however, they have the drawback that they decohere N times faster than a single spin since they always accumulate a collective phase. The fast decoherence rate of these states, however, is not problematic in our case since the GHZ state is prepared along the x direction where most of the population is distributed close to the $|M|=0$ levels.

Quantitatively the effect of decoherence can be calculated by using the uncoupled spin basis as it diagonalizes the total Hamiltonian. Each state in this basis can be labeled as $\{|n^{(k)}\rangle = |s_1^k, s_2^k, \dots, s_N^k\rangle\}$, where $s_i^k = \pm 1$ for $\uparrow\downarrow$ and $k = 1, \dots, 2^N$.

If at $t=0$ the reduced density matrix of the system, $\hat{\rho}$, is given by $\hat{\rho} = \sum_{k,l} \rho_{k,l}(0) |n^{(k)}\rangle \langle n^{(l)}|$, after time t ,

$$\rho_{k,l}(t) = \rho_{k,l}(0) e^{i/4\chi t [(\sum_{i=1}^N s_i^k)^2 - (\sum_{i=1}^N s_i^l)^2]} e^{-i\sum_{i=1}^N \int_0^t d\tau \theta_i(\tau) (s_i^k - s_i^l)}. \quad (5)$$

As a consequence, $\langle \hat{J}_x^{(0)}(t) \rangle = \text{Tr}[\hat{J}_x^{(0)} \hat{\rho}(t)] = e^{-\Gamma(t)} \langle \hat{J}_x^{(0)}(t) \rangle|_{\Gamma=0}$ with $\langle \hat{J}_x^{(0)}(t) \rangle|_{\Gamma=0}$ the expectation value in the absence of noise [Eq. (2)]. The factor $e^{-\Gamma(t)}$ comes from the fact that the operator $\hat{J}_x^{(0)} = \sum_i \hat{\sigma}_i^x$ only probes one-particle coherence, i.e., it only connects states with exactly one spin flipped.

Since at $t=0$ all atoms are polarized in the x direction, i.e., $\rho_{k,l}(0) = 2^{-N}$, one can show from Eq. (5) that the fidelity is degraded to

$$\mathcal{F}(t_0) = \frac{1}{2^{2N}} \sum_{l,k} e^{-\Gamma(t_0) \sum_{i=1}^N (s_i^k - s_i^l)^2} = \left(\frac{1 + e^{-\Gamma(t_0)}}{2} \right)^N. \quad (6)$$

III. PROTECTED DYNAMICS

A. Many-body protected manifold

Let us now consider what happens if in addition to \hat{H}_z we assume that there is isotropic infinite-range ferromagnetic interactions between the spins, so the system is described by the Hamiltonian

$$H_c = \hat{H}_{\text{prot}} + \hat{H}_z,$$

$$\hat{H}_{\text{prot}} = -\lambda \hat{J}^{(0)2}. \quad (7)$$

The isotropic Hamiltonian \hat{H}_{prot} has a ground-state manifold spanned by a set of $N+1$ degenerate states. They lie on the surface of the Bloch sphere with maximal radius $J=N/2$ and are totally symmetric, i.e., invariant with respect to particle permutations. There is a finite-energy gap $E_g = \lambda N$ that isolates the ground-state manifold from the rest of the Hilbert space. This gap is the key for the many-body protection against decoherence. Here, we will refer to the ground-state manifold as the many-body protected manifold (MPM).

B. Protection against phase decoherence

The low-energy spectrum of \hat{H}_c is shown in Fig. 3. As \hat{H}_z commutes with \hat{H}_{prot} , in the absence of decoherence the latter does not affect at all the GHZ generation dynamics, however in the presence of decoherence the latter does significantly reduce the effect of local environmental noise. While \hat{H}_{prot} significantly reduces the environment decoherence it does not affect the system dynamics since, within the MPM, \hat{H}_{prot} acts as a constant term. The protection can be best understood by using the basis of collective states. In terms of collective spin operators \hat{H}_{env} can be written as

$$\hat{H}_{\text{env}} = \frac{1}{\sqrt{N}} \sum_{k=0}^{N-1} g^k(t) \hat{J}_z^{(k)}, \quad (8)$$

where $g^k(t) = \frac{1}{\sqrt{N}} \sum h_j(t) e^{-i2\pi jk/N}$ and $\hat{J}_z^{(k)} = \frac{1}{2} \sum \hat{\sigma}_j^\alpha e^{i2\pi jk/N}$. Note that allowed transitions must conserve M as both the system and noise Hamiltonian commute with $\hat{J}_z^{(0)}$. In the presence of a large energy gap E_g , one can distinguish two different type of processes: (i) Decoherence effects that take place within the MPM due to the collective dynamics induced by the $k=0$ component of \hat{H}_{env} , and (ii) transitions across the gap induced by the inhomogeneous terms. The later couple the MPM with the rest of the system, however they are a non-energy conserving process and consequently perturbatively weak.

Using a perturbative analysis, and assuming that at $t=0$ the system lies within the MPM, the evolution of the projection of the density matrix on the MPM, $\rho_{M\tilde{M}} \equiv \langle N/2, \tilde{M} | \hat{\rho} | N/2, M \rangle_z$, can be written as

$$\rho_{M,\tilde{M}}(t) = \rho_{M,\tilde{M}}(0) e^{i\chi(M^2 - \tilde{M}^2)} e^{i(\theta_M - \theta_{\tilde{M}})} e^{-1/2(\gamma_M - \gamma_{\tilde{M}})}. \quad (9)$$

Here,

$$\theta_M(t) \equiv \left\langle \frac{N}{2}, M \left| \int_0^t d\tau \hat{H}_{\text{env}}(\tau) \right| \frac{N}{2}, M \right\rangle = \frac{M}{\sqrt{N}} \int_0^t g^0(\tau) \quad (10)$$

accounts for the dynamics induced by the noise within the MPM and

$$\gamma^M(t) = \sum_{J \neq N/2, \beta} \left| \int_0^t d\tau \mathcal{M}_{J,\beta}^M e^{i\tau\omega_{J,\beta}} \right|^2, \quad (11)$$

takes into account the depletion of the $J=N/2$ levels due to transition matrix elements between $|\frac{N}{2}, M\rangle_z$ and states outside the MPM, $\mathcal{M}_{J,\beta}^M = \langle \frac{N}{2}, M | \hat{H}_{\text{env}} | J, M, \beta \rangle_z$. $\omega_{J,\beta}$ are the respective energy splittings. Because \hat{H}_{env} is a vector operator, according to the Wigner-Eckart theorem, \hat{H}_{env} only couples the states in the MPM with states which have $J=N/2-1$ and thus with excitation energy λN .

Assuming the power spectrum of the noise, $f(\omega) \equiv \int dt e^{-i\omega t} f(t)$, to have a cutoff frequency ω_c [e.g., $f(\omega) = f$ for $\omega \leq \omega_c$ and 0 otherwise], we find that

$$\overline{\gamma^M(t)} \approx \frac{N^2 - 4M^2}{N} f \int_0^{\omega_c} d\omega \left(\frac{\sin[t(\omega - E_g)/2]}{\omega - E_g} \right)^2. \quad (12)$$

In the limit when the noise is sufficiently slow, i.e., $\omega_c \ll E_g$, then $\overline{\gamma^M(t)}$ is bounded for all times, $\overline{\gamma^M(t)} < \left(\frac{N^2 - 4M^2}{N^2} \right) \left(\frac{f\omega_c}{\lambda E_g} \right) \ll 1$, and the atomic population within the ground-state manifold is fully preserved, i.e., $\gamma^M(t) \approx 0$ in Eq. (9).

Consequently, in the slow noise limit type (ii) processes are energetically forbidden and only type (i) processes are effective and therefore the noise acts just as a uniform random magnetic field: If at $t=0$ $\hat{\rho} = \sum_{M,\tilde{M}} \rho_{M,\tilde{M}}(0) |\frac{N}{2}, \tilde{M}\rangle \langle \frac{N}{2}, M|$, then after time t each component $\rho_{M,\tilde{M}}$ acquires an additional random phase $e^{i[\theta_M(t) - \theta_{\tilde{M}}(t)]}$ and on average

$$\overline{\rho_{M,\tilde{M}}(t)} = \rho_{M,\tilde{M}}(0) e^{i\chi t(M^2 - \tilde{M}^2)} e^{-\Gamma(t)(M - \tilde{M})^2/N}. \quad (13)$$

The factor of \sqrt{N} in the denominator of θ_M is fundamental for the reduction of the effect of decoherence within the MPM. For example, it makes $\hat{J}_{x,y}^{(0)}$ decay N times slower than in the unprotected system, i.e., $\langle \hat{J}_{x,y}^{(0)}(t) \rangle = e^{-\Gamma(t)/N} \langle \hat{J}_{x,y}^{(0)}(t) \rangle_{\Gamma=0}$.

Assuming all atoms are initially polarized in the x direction, $\rho_{M,\tilde{M}}(0) = 2^{-N} \sqrt{\binom{N}{M+N/2} \binom{N}{\tilde{M}+N/2}}$, using Eq. (13), the approximation $\binom{N}{M+N/2} \approx \left(\frac{2}{\pi N}\right)^{1/4} e^{-M^2/N}$, valid in the large N limit and replacing the sums over M and \tilde{M} by integrals the fidelity at a time t can be shown to be given by

$$\mathcal{F}(t_0) = \frac{1}{\sqrt{1 + \Gamma(t_0)}}. \quad (14)$$

The insensitivity of $\mathcal{F}(t)$ on N , and the N times slower decay rate of $\langle \hat{J}_x^{(0)} \rangle$ demonstrate the usefulness of MPM to generate a large number of entangled particles.

C. Protection against arbitrary noise

We now discuss the protection against spin flips, which can be modeled by terms proportional to σ_i^x , σ_i^y in the noise Hamiltonian, Eq. (4). First, note that as the \uparrow and \downarrow states have a finite-energy splitting ω_0 , low-frequency noise associated with such terms will be suppressed. However, most of the spin flips are generally induced by imperfections in the laser fields and therefore are at frequencies close to ω_0 , i.e., they correspond to low-frequency noise in the rotating frame of the laser. In the case involving GHZ state generation, the finite-energy cost imposed by χJ_z^2 between levels with different $|M|$ value tends to inhibit these processes as illustrated in Fig. 2. If in addition \hat{H}_{prot} is present, this natural protection can be enhanced due to the fact that the energy gap suppresses the component of the noise that causes transitions between the MPM and other manifolds. More precisely, noise modeled as $\sum_i h^\alpha \hat{\sigma}_i^\alpha$, when projected into the MPM reduces to $\frac{1}{\sqrt{N}} g_\alpha^0(t) \hat{J}_\alpha^0$ with $\alpha = x, y, z$.

In Fig. 4 we quantify the protection provided by the MPM. In the absence of any protection we find the finite-energy cost imposed by H_z helps to protect the system against transversal noise. Instead of the exponential decay ($\sim e^{-N\Gamma(t_0)}$) of the fidelity observed when dephasing is present, spin flips degrade the fidelity as $\sim e^{-\Gamma(t_0)N/4}$ (at least for the moderated $N < 12$ we must restrict our simulations). With protection the fidelity scales even better as the transversal noise is restricted to act only within the MPM. Instead of the exponential decay of the GHZ generation fidelity with N , with protection it decays as $\sim e^{-A\Gamma(t_0)N^{0.44}}$ with A a numerical constant, $A \sim 1/3$ (for this result we do not have to restrict to moderated N). Hence, with \hat{H}_{prot} we gain a factor of order $\sim \sqrt{N}$. The reason why \hat{J}_x^0 and \hat{J}_y^0 noise degrade stronger the fidelity than \hat{J}_z^0 noise (which leads just to a N -independent fidelity) is that the former do not commute with \hat{H}_z and mix states with different M quantum number. Additionally, in the

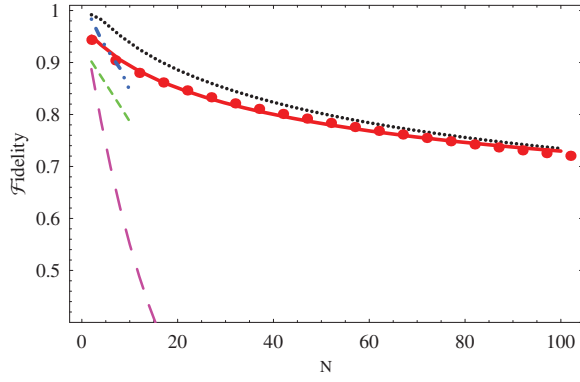


FIG. 4. (Color online) Fidelity to create GHZ state as a function of N for systems in the presence of σ_y noise: without MPM (green dashed line), without MPM but with spin echo (dotted-dashed blue line), with MPM (red solid line), and with both MPM and echo (dotted black line). We also show the degradation caused by pure dephasing in an unprotected system (long dashed purple line) for comparison purposes. For simplicity we assumed infinite correlation time, $f(\omega) = Y\delta(\omega/\chi)$, $Y = 0.1\chi$. The echo technique consisted of a perfect sudden π pulse around the x direction at $\chi t = \pi/4$. Because the y components of the noise do not commute with $\hat{J}_z^{(0)}$ the dynamics was solved numerically. For the unprotected system all the 2^N states must be considered and we must limit the particle number by $N = 10$. On the other hand, the restriction of the dynamics to the MPM in the protected scheme allowed us to extend the calculation to larger N values. For the σ_y noise the fidelity with protection does not become N independent, but instead scales as $e^{-0.043N^{0.44}}$ (see fitted red dots). Nevertheless we do gain a factor of order \sqrt{N} with respect to the unprotected system. The plot also shows that the combination of MPM with spin echo provides the best protection.

figure we show that for noise with long correlation time the use of spin-echo techniques can help to further reduce the effect of decoherence.

IV. IMPLEMENTATION OF THE GAP PROTECTED HAMILTONIAN IN TRAPPED IONS

A. Ideal conditions

We now proceed to review and complement the implementation of the protected Hamiltonian, $\chi(\hat{J}^{(0)2} - \hat{J}_z^{(0)2})$, proposed in Ref. [14]. Consider a linear trap with a string of ions in two relevant internal levels. The ions are assumed to be cooled such that only the in-phase collective center-of-mass oscillation of all ions is excited. The corresponding oscillation frequency is denoted by ν . The two internal levels of the ions are coupled by a monochromatic laser field with slowly varying Rabi frequencies Ω and with frequency $\omega_1 = \omega_0 + \delta$, where δ is the detuning from resonance (see Fig. 5). Assuming that the field couples all ions in the same way, we can describe the system by the Hamiltonian $\hat{H} = \hat{H}_0 + \hat{H}_{in}$, with

$$H_0 = \nu \hat{a}^\dagger \hat{a} + \omega_0 \hat{J}_z^{(0)}, \quad (15)$$

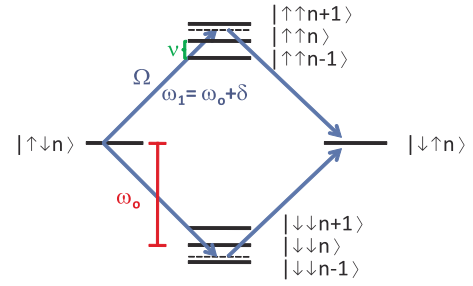


FIG. 5. (Color online) Energy-level diagram for a pair of ions illuminated by a monochromatic beam with detuning δ from the atomic transition. The quantity n denotes the quantum number of trap oscillations with frequency ν . δ is assumed to be large compared to the linewidth of the resonance and consequently the dominant processes are two-photon transitions. These transitions lead to a collective Hamiltonian for the many-ion system of the form $\chi(\hat{J}^{(0)2} - \hat{J}_z^{(0)2})$.

$$\hat{H}_{in} = \Omega \hat{J}_+^{(0)} e^{i\delta t} e^{i\eta(\hat{a}^\dagger e^{i\nu t} + \hat{a} e^{-i\nu t})} + \text{H.c.}, \quad (16)$$

where \hat{a} is the annihilation operator of the quantized oscillation mode, η is the Lamb-Dicke parameter. The detuning δ is assumed to be large compared to the linewidth of the resonance, γ_R , but sufficiently different from the frequency of the center-of-mass oscillation, i.e., $|\delta|, |\nu \pm \delta| \gg \gamma_R$. As a consequence, the dominant processes are two-photon transitions leading to a simultaneous excitation of pairs of ions, see Fig. 5.

We first assume that the ion trap is in the Lamb-Dicke limit, i.e., that the ions are cooled sufficiently enough, such that all relevant excitation numbers n of the trap oscillation $(n+1)\eta^2 \ll 1$ hold. In this limit one can expand the exponent in Eq. (16) to first order in η . Confining the interest to time-averaged dynamics over a period much longer than any of the oscillations present in \hat{H}_{in} , the oscillatory terms may be neglected and we are left with a more simple effective Hamiltonian (see Ref. [15] for derivation details),

$$H_{\text{eff}} = \chi(\hat{J}^{(0)2} - \hat{J}_z^{(0)2}) + \left(\frac{2\nu\eta^2\Omega^2}{\delta - \nu^2} + \Lambda \right) \hat{J}_z^{(0)} + 2\Lambda n \hat{J}_z^{(0)}, \quad (17)$$

where $\chi = \frac{2\nu\eta^2\Omega^2}{\delta - \nu^2}$, $\Lambda = \frac{\chi\delta}{\nu}$. The first term in H_{eff} is the desired protected Hamiltonian. The second term acts as an effective magnetic field which can be canceled by adding an external magnetic field or by echo techniques. The third term comes from the ac Stark shift of the atomic levels due to the laser fields.

We will now, quantify the advantage of using the MPM for a realistic experimental parameter. First we assume all ions are in the vibrational ground state and ideal conditions, i.e., $H_{\text{eff}} = \hat{H}_c$, and then proceed to discuss deviations from the ideal situation. We consider the experimental parameters of Ref. [3], and identify the spin \uparrow and \downarrow levels with the $2s^2S_{1/2}$ hyperfine states $|F=2, m_F=-2\rangle$ and $|F=2, m_F=-1\rangle$ of ${}^9\text{Be}^+$ ions trapped in a linear Pauli trap with an axial center-of-mass frequency $\nu = 2\pi \times 3.86$ MHz. Choosing $\delta \sim 1.2\nu$, $\eta \sim 0.15$, and not too strong laser intensities $\Omega = 0.1\nu$, so that a negligible population is transferred to intermediate vibra-

tional levels, we estimate $|\lambda|=|\chi|=25$ kHz and a GHZ preparation time $t_o=63$ μ s. In Ref. [16], it was determined that in typical laboratory conditions the random magnetic field changes are of the order of 0.1 μ T with a qubit transition depending linearly on the magnetic field with a coefficient of approximately 21 kHz/ μ T. With these parameters we obtain that the fidelity of the GHZ state in the absence of protection [see Eq. (6)], is degraded even for six ions to $\mathcal{F}=0.75$ (dotted black line in Fig. 1). On the other hand, using the MPM, the fidelity improves to $\mathcal{F}=0.95$ (solid red line in Fig. 1). For this implementation of H_{prot} it is important to mention that whereas the GHZ fidelity does not explicitly depend on N [see Eq. (14)], it implicitly depends on it due to the fact that λ decreases with N as $\sqrt{\ln N/N}$. The reason for this dependence is that in an effective one-dimensional (1D) ion chain there is a critical ratio between the axial and transversal trapping frequencies $\alpha_{\text{crit}}=v^2/v_{T,\text{crit}}^2=16 \ln N/(9N^2)$, at which the ions become unstable (see Ref. [17] for details) and thus λ scales as $v_{T,\text{crit}}\sqrt{\ln N/N}$. This dependence however does not affect the protection mechanism since the gap, E_g , grows as $\sqrt{\ln N}$.

Since the present implementation of \hat{H}_c yields always $|\lambda|=|\chi|$ a relevant question is, if it is possible to implement in these systems \hat{H}_{prot} and \hat{H}_z independently. A possible way to do so is to use the Mølmer and Sørensen [7] proposal for implementing $\hat{H}_z=\chi\hat{J}_z^{(0)2}$ via virtual vibrational excitations with bichromatic beams and to combine it with multiple resonant pulses that rotate the Bloch vector: A resonant $\pi/2$ pulse acting simultaneously on all ions rotates the $\hat{J}_z^{(0)}$ operator into $\hat{J}_y^{(0)}$. Hence, by applying $\pi/2$ pulses, in conjunction with the Mølmer and Sørensen scheme, it is possible to turn \hat{H}_z into \hat{H}_y . Similarly \hat{H}_x can be implemented. Because the different \hat{H}_α do not commute, it is not possible to realize \hat{H}_{prot} by simply applying \hat{H}_z for the desired time t , followed by \hat{H}_y and \hat{H}_x . Instead one needs to stroboscopically apply the various Hamiltonians for short time steps dt so that the commutation error becomes only of order $\propto dt^2$. This procedure, which is just a practical application of the Trotter approximation, will lead to an effective implementation of \hat{H}_{prot} . The drawback however is that if the time step dt is not short enough, it can lead to additional decoherence errors during the dynamical evolution.

B. Applications to precision measurements using trapped ions

Recent experiments [3,4] have generated GHZ states made of up to six beryllium ions and used them to perform precision measurements of ω_0 . For the ideal GHZ state preparation, the spectroscopy should lead to Heisenberg-limited resolution, $|\delta\omega_0|\propto N^{-1}$ [11]. However, in practice, even for six ions, the phase accuracy was significantly degraded by decoherence.

The spectroscopy [3,4] was realized by first creating the desired GHZ state by applying to the initial polarized state, $|J=N/2, N/2\rangle_z$, the unitary gate operation $U_N=e^{i\pi/2J_y^{(0)}}e^{i\pi/2J_z^{(0)2}}e^{-i\pi/2J_y^{(0)}}$. Then, the GHZ state was let to freely precess in the z direction for time t so each atom

accumulated a phase difference $\phi=(\omega-\omega_0)t$ (in a reference frame rotating with the frequency ω , the frequency of the applied field). The phase difference was then decoded by measuring the collapse probability into the states $|J=N/2, N/2\rangle_z$ or $|J=N/2, -N/2\rangle_z$ after applying the unitary transformation $\prod_i\sigma_i^x$.

This generalized Ramsey sequence can be quantitatively described as a measure of the expectation value of the following operator, \hat{O} :

$$\langle\hat{O}\rangle=\langle\psi(t_0)|\prod_i[\cos(\phi)\hat{\sigma}_i^z-\sin(\phi)\hat{\sigma}_i^y]|\psi(t_0)\rangle \quad (18)$$

with $|\psi(t_0)\rangle=e^{-i\pi/2J_z^{(0)2}}|N/2, N/2\rangle_x$.

The phase sensitivity $\langle\Delta^2\hat{O}\rangle$ achievable by repeating the above scheme during total time T is related to the signal variance $\langle\Delta^2\hat{O}\rangle=\langle\hat{O}^2\rangle-\langle\hat{O}\rangle^2$ and given by $|\delta\omega_0|=\sqrt{\frac{1}{iT}\frac{\langle\Delta^2\hat{O}\rangle}{\langle\hat{O}\rangle^2}}$ [12]. Because $\hat{O}^2=1$, we only need to calculate $\langle\hat{O}\rangle=\text{Tr}[\hat{\rho}(t_0)\hat{O}]$ to evaluate $\delta\omega_0$.

Experimentally, magnetic field noise is one of the sources of phase decoherence. Assuming that such dephasing mainly takes place during the GHZ generation, as during the Ramsey interrogation time the atoms are essentially freely evolving, using Eq. (5) one can show that for the unprotected system

$$\begin{aligned} \langle\hat{O}\rangle &= \langle\psi_x^{\text{GHZ}}|\prod_i[\cos(\phi)\hat{\sigma}_i^z-e^{-\Gamma(t_0)}\sin(\phi)\hat{\sigma}_i^y]|\psi_x^{\text{GHZ}}\rangle \\ &= \frac{1}{2}\left(\frac{e^{i\phi}(1-e^{-\Gamma(t_0)})+e^{-i\phi}(1+e^{-\Gamma(t_0)})}{2}\right)^N + \text{H.c.} \end{aligned} \quad (19)$$

Consequently the maximal phase resolution, achieved at $\phi_{\text{opt}}=n\pi$ (for integer n), can be shown to be given by

$$|\delta\omega_0|_{\text{opt}}=|\delta\omega_0|_{\text{sh}}/G, \quad (20)$$

with $G=\sqrt{[(N-1)e^{-2\Gamma(t_0)}+1]}$ and $|\delta\omega_0|_{\text{sh}}=\frac{1}{\sqrt{tN}}$ the shot-noise resolution. The factor G explains the strong limitations introduced by decoherence. In the limiting case that the time required to generate the GHZ state is slow enough that $G\sim 1$ [i.e., when $\Gamma(t_0)>\ln(\sqrt{N})$], the phase accuracy is reduced to the classical shot-noise resolution. However, if instead \hat{H}_c is used for the GHZ generation, G is replaced by $\sqrt{[(N-1)e^{-2\Gamma(t_0)/N}+1]}$. Due to the N times slower decay rate of the atomic coherences, the same preparation time that leads to shot-noise resolution without protection, can lead to a much higher sensitivity with protection.

In Fig. 6 we plot $|\delta\omega_0|_{\text{opt}}$ using realistic experimental parameters and compare the achievable sensitivity with and without protection. The figure shows an enhancement in sensitivity up to 30% even for the few ions in consideration.

C. Nonideal conditions

So far we have used the Lamb-Dicke and the rotating-wave approximation. Now we perform a more detailed analysis of the validity of these approximations and estimate the effect of deviations from the ideal situation in an actual experiment.

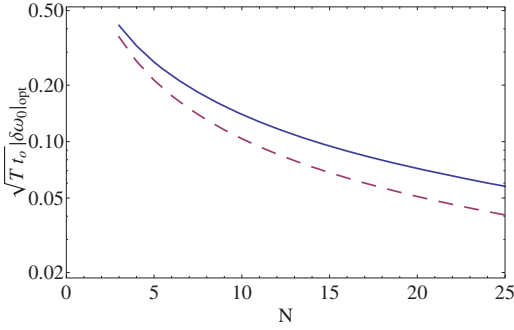


FIG. 6. (Color online) Phase sensitivity in precision spectroscopy with trapped ions as a function of N . The vertical axis is in a logarithmic scale. We used the same parameters as Fig. 1 for the noise $\chi=25$ kHz, $\Omega=0.05\nu$, and $\nu=2\pi\times 3.86$ MHz. The blue line shows the phase sensitivity without protection [Eq. (20)] and the red dashed line with protection. Even with these reduced number of ions we observe up to a 30% improvement.

1. Finite temperature

The Sørensen and Mølmer scheme used to create $\hat{J}_z^{(0)2}$, leads to an effective Hamiltonian independent of vibration quantum numbers due to the destructive interference of the transition paths to intermediate vibrational states that the two applied laser frequencies provide. On the contrary, our implementation of \hat{H}_c , which requires a monochromatic beam, lacks the desired cancellation and a term proportional to $2\Lambda n \hat{J}_z^{(0)}$, appears in the effective Hamiltonian, see Eq. (17). This term, if not corrected, can certainly degrade the fidelity to

$$\mathcal{F}(t_o) = \sum_n P_n \exp\left(-\frac{N^2 \Lambda^2 (2n)^2 t_o^2}{8}\right) \sim 1 - \frac{\bar{n}}{\bar{n}+1}, \quad (21)$$

where P_n is the initial population of the state with n phonons and \bar{n} is the mean vibrational quanta. For a thermal state with $\bar{n}=1$, $\mathcal{F}(t_o) \sim 0.5$, which is quite low. In order to prevent this effect one must cool the ions to the ground state, $P_n = \delta_{n0}$, which is feasible with the state-of-the-art technology. Alternatively one can use spin-echo techniques. For example, if at time $t_o/2$ the sign of the laser detuning δ is changed, then the different components will rotate in the opposite direction and at t_o the net effect due to the extra second and third terms in \hat{H}_{eff} will be canceled out. Assuming this cancellation, we proceed to estimate the small nonideal deviations by using perturbation theory.

2. Direct coupling

Going from Eq. (16) to Eq. (17) the off-resonant term $H_d = \Omega \hat{J}_+^{(0)} e^{i\delta} + \text{H.c.}$ was neglected. This term corresponds to direct single atom spin flips without any vibrational excitation.

Changing to the interaction picture of H_{eff} and using the fact that H_d oscillates to a much higher frequency than $\hat{U}(t) = e^{iH_{\text{eff}}t}$, so that the latter can be treated as constant in the integrals used in the Dyson series, one can show that

$$\mathcal{F}(t_o) = 1 - \frac{\Omega^2}{\delta^2} [N^2 \sin^2(\delta t_o) + 4N \sin^4(\delta t_o/2) + \dots]. \quad (22)$$

The degradation of fidelity is a factor of N larger than the degradation caused by direct couplings in the standard realization of $J_z^{(0)2}$, where $\mathcal{F}(t_o) = 1 - \frac{N\Omega^2}{\delta^2} \sin^2(\delta t_o)$. Even for six ions, using a modest Rabi frequency $\Omega=0.1\nu$, $t_o=63 \mu\text{s}$, $\delta \sim 1.2\nu$, and $\nu=2\pi\times 3.86$ MHz, this effect can cause significant loss in fidelity, $\mathcal{F}(t_o) \sim 0.75$. Therefore, it is important for the implementation of the protected Hamiltonian to use weak laser power and to control the system parameter such that $\delta t_o = 2K\pi$ with K as an integer.

3. Lamb-Dicke approximation

In Ref. [8] it has been shown that relaxing the Lamb-Dicke approximation and including higher order terms results in an effective χ_n which depends on the vibrational number of phonons in the collective mode, $\chi_n = \chi [1 - \eta^2(2n+1) + \eta^4(5/4n^2 + 5/4n + 1/2)]$. As this effect is global, the gap does not protect against it and it leads to a degradation of the fidelity given by

$$\begin{aligned} \mathcal{F}(t_o) &= \sum_n P_n \left(1 + \frac{N(N-1)(\pi/2 - \chi_n t_o)^2}{4}\right)^{-1/2} \\ &\sim 1 - \frac{\pi^2 N(N-1)\eta^4}{32} \sum_n P_n (2n+1)^2. \end{aligned} \quad (23)$$

Assuming a typical Lamb-Dicke parameter of order $\eta \sim 0.15$ and ground-state cooling, these corrections limit the number of ions to less than 40 if one requires a degradation in fidelity no greater than 30%.

4. Other vibrational modes

With N ions in the trap, assuming that the transversal potential is strong enough to freeze the transversal degree of freedom, only the N longitudinal vibrational modes are relevant. So far we have assumed that only the collective center-of-mass motion is excited and neglected other modes. If we include the effect of other modes, the fidelity is decreased. The main sources of decoherence are (a) off-resonant direct couplings to other modes and (b) reduction of the coupling to the center-of-mass mode, χ , due to the vibration of the other modes. However, all of these effects are local and the gap energetically suppresses them.

5. Spontaneous emission

Another fundamental source of decoherence arises from spontaneous emission effects. In typical ion-trap experiments the $|\uparrow\rangle$ and $|\downarrow\rangle$ levels are coupled through Raman transitions to a third excited level $|e\rangle$. We denote by $\nu_1(\nu_2)$ the energy splitting between $|\downarrow\rangle$ ($|\uparrow\rangle$) and $|e\rangle$ (see Fig. 7). Assuming two-photon resonance conditions, that is $\omega_{e1} - \omega_{e2} = \nu_1 - \nu_2 = \omega_0$ and $\Delta = \omega_{e1} - \nu_1 = \omega_{e2} - \nu_2$, where Δ is the detuning of the fields from the one-photon resonance, $\omega_{e1,2}$ and $\Omega_{1,2}$ are laser frequencies and Rabi frequencies, respectively, the Hamil-

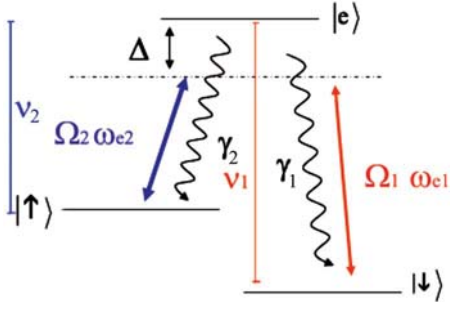


FIG. 7. (Color online) Raman transition to a third level with atomic decay. Here Δ is the detuning of the laser fields with frequencies $\omega_{e1,2}$ from the one-photon resonances with frequencies $\nu_{1,2}$, i.e., $\Delta = \omega_{e1} - \nu_1 = \omega_{e2} - \nu_2$, and $\Omega_{1,2}$ are laser Rabi frequencies.

tonian of the system in the appropriate rotating frame can be written as

$$\hat{H}_s = -\Delta \sum_i \hat{\sigma}_{ee}^i + \hat{H}_{Is}, \quad (24)$$

$$\hat{H}_{Is} = \Omega_1 \sum_i (\hat{\sigma}_{\downarrow e}^i + \hat{\sigma}_{e\downarrow}^i) + \Omega_2 \sum_i (\hat{\sigma}_{\uparrow e}^i + \hat{\sigma}_{e\uparrow}^i), \quad (25)$$

where $\hat{\sigma}_{ee}^i = |e\rangle_i \langle e|$, $\hat{\sigma}_{\downarrow e}^i = |\downarrow\rangle_i \langle e|$, and $\hat{\sigma}_{\uparrow e}^i = |\uparrow\rangle_i \langle e|$.

The decoherence processes due to spontaneous emission can be described by means of Heisenberg-Langevin equations [19] given by

$$\dot{\hat{\sigma}}_{\downarrow\downarrow}^j = (i\Omega_1 + \hat{f}_{\downarrow e}^{j\dagger}) \hat{\sigma}_{\downarrow e}^j - (i\Omega_2 - \hat{f}_{\uparrow e}^j) \hat{\sigma}_{e\downarrow}^j, \quad (26)$$

$$\begin{aligned} \dot{\hat{\sigma}}_{\uparrow e}^j = & -(i\Delta + \Gamma_e/2) \hat{\sigma}_{\uparrow e}^j - (i\Omega_2 - \hat{f}_{\uparrow e}^j) (\hat{\sigma}_{ee}^j - \hat{\sigma}_{\uparrow\uparrow}^j) \\ & + (i\Omega_1 - \hat{f}_{\downarrow e}^j) \hat{\sigma}_{\downarrow\downarrow}^j, \end{aligned} \quad (27)$$

$$\dot{\hat{\sigma}}_{e\downarrow}^j = (i\Delta - \Gamma_e/2) \hat{\sigma}_{e\downarrow}^j + (i\Omega_1 + \hat{f}_{\downarrow e}^{j\dagger}) (\hat{\sigma}_{ee}^j - \hat{\sigma}_{\downarrow\downarrow}^j) \quad (28)$$

$$- (i\Omega_2 + \hat{f}_{\uparrow e}^{j\dagger}) \hat{\sigma}_{\uparrow\uparrow}^j, \quad (29)$$

where $\Gamma_e = \gamma_1 + \gamma_2$ with γ_1 and γ_2 are decay rates from $|e\rangle$ to $|\downarrow\rangle$ and $|\uparrow\rangle$, respectively, and the noise operators \hat{f} have zero mean and are δ correlated: $\langle \hat{f}_{\downarrow e}^j(t) \hat{f}_{\downarrow e}^{k\dagger}(t') \rangle = \gamma_1 \delta(t-t') \delta_{j,k}$ and $\langle \hat{f}_{\uparrow e}^j(t) \hat{f}_{\uparrow e}^{k\dagger}(t') \rangle = \gamma_2 \delta(t-t') \delta_{j,k}$.

In the large photon detuning limit $\Delta \gg \Omega_1 \Omega_2, \gamma_1, \gamma_2$, one can adiabatically eliminate the operators $\hat{\sigma}_{e\downarrow}^j$ and $\hat{\sigma}_{e\uparrow}^j$ and their Hermite conjugates and then use the projected equations of motion to solve for $\hat{\sigma}_{\downarrow\downarrow}^j$,

$$\dot{\hat{\sigma}}_{\downarrow\downarrow}^j = FH + i[\hat{H}_{\text{noise}}, \hat{\sigma}_{\downarrow\downarrow}^j], \quad (30)$$

$$\hat{H}_{\text{noise}}(t) = \frac{1}{2} \sum_j [h_{jz}^s(t) \hat{\sigma}_j^z + h_{jx}^s(t) \hat{\sigma}_j^x + h_{jy}^s(t) \hat{\sigma}_j^y], \quad (31)$$

where FH accounts for the Hamiltonian part of the dynamics and

$$h_{jz}^s(t) = \frac{\Omega_1}{i\Delta} (\hat{f}_{\downarrow e}^{j\dagger} - \hat{f}_{\downarrow e}^j) - \frac{\Omega_2}{i\Delta} (\hat{f}_{\uparrow e}^{j\dagger} - \hat{f}_{\uparrow e}^j), \quad (32)$$

$$h_{jx}^s(t) = -\frac{\Omega_2}{i\Delta} (\hat{f}_{\downarrow e}^{j\dagger} - \hat{f}_{\downarrow e}^j) - \frac{\Omega_1}{i\Delta} (\hat{f}_{\uparrow e}^{j\dagger} - \hat{f}_{\uparrow e}^j), \quad (33)$$

$$h_{jy}^s(t) = -\frac{\Omega_2}{\Delta} (\hat{f}_{\downarrow e}^{j\dagger} + \hat{f}_{\downarrow e}^j) + \frac{\Omega_1}{\Delta} (\hat{f}_{\uparrow e}^{j\dagger} + \hat{f}_{\uparrow e}^j). \quad (34)$$

From the previous expressions one can estimate the degradation of the fidelity due to dephasing (similar degradation of the fidelity is caused by x or y types of noise). In the adiabatic limit, i.e., $\Delta \gg \Omega_1 \Omega_2, \gamma_1, \gamma_2$, h_{jz}^s are independent stochastic white-noise processes with zero mean and autocorrelation function $\overline{h_{jz}^s(t) h_{jz}^s(\tau)} = \gamma_{sp} \delta_{ij} \delta(t-\tau)$ with $\gamma_{sp} = \frac{(\gamma_1 \Omega_1^2 + \gamma_2 \Omega_2^2)}{\Delta^2}$. Consequently the gap cannot protect against this broad band noise and according to Eq. (6) they will cause a degradation of the GHZ fidelity given by

$$\mathcal{F} = 1 - \frac{\gamma_{sp} N t_o}{4}. \quad (35)$$

In current experiments spontaneous emission is one fundamental source of decoherence. For the particular case of Ref. [4], with a gate duration time $t_o \sim 50 \mu\text{s}$, they estimated for six ions an 18% probability of spontaneous emission per gate. In order to reduce the strong degradations due to this type of high-frequency decoherence process one can increase the Raman detuning [18] at the expense of slower evolution which in turn will make the system more susceptible to other kind of local noise (e.g., magnetic field inhomogeneities). On the other hand, the latter can be suppressed by the MPM.

From this analysis we conclude that overhead of implementing $\hat{J}^{(0)2} - \hat{J}_z^{(0)2}$ instead of $\hat{J}_z^{(0)2}$ is mainly the additional echo technique required to remove the n dependence of H_{eff} . Besides that, on average the same type of nonideal disturbances are found in both Hamiltonians with the advantage of $\hat{J}^{(0)2} - \hat{J}_z^{(0)2}$ that the gap protects the system against those of them which are local in character.

V. IMPLEMENTATION IN OPTICAL LATTICES

A. Engineering long-range interactions

Up to now we have explored only the generation of an MPM via isotropic long-range interactions. In practice, however, it is desirable to have a similar kind of protection generated by systems with short-range interactions such as those provided by cold atoms in optical lattices. These systems offer the possibility to dynamically change the Hamiltonian parameters at a level unavailable in more traditional condensed matter systems. We now show how an MPM can be created in lattice systems and can be used to robustly generate N -particle GHZ states.

We consider ultracold bosonic atoms with two relevant internal states confined in an optical lattice. We will assume that the lattice is loaded with one atom per site, and again identify the two possible states of each site, with the effective spin index $\sigma = \uparrow, \downarrow$, respectively. For deep periodic potential and low temperatures, the atoms are confined to the lowest Bloch band and the low-energy Hamiltonian is given by [20]

$$\begin{aligned} \hat{H}_{BH} = & -\tau \sum_{\langle i,j \rangle \sigma} \hat{a}_{\sigma,i}^\dagger \hat{a}_{\sigma,j} + \frac{1}{2} \sum_{j\sigma} U_{\sigma\sigma} [\hat{n}_{\sigma,j} (\hat{n}_{\sigma,j} - 1)] \\ & + \sum_j U_{\uparrow\downarrow} \hat{n}_{\uparrow,j} \hat{n}_{\downarrow,j}. \end{aligned} \quad (36)$$

Here $\hat{a}_{\sigma,j}$ are bosonic annihilation operators of a particle at site j and state σ , $\hat{n}_{\sigma,j} = \hat{a}_{\sigma,j}^\dagger \hat{a}_{\sigma,j}$, and the sum $\langle i,j \rangle$ is over nearest neighbors. In Eq. (36) the parameter τ is the tunneling energy between adjacent sites (which we assume spin independent) and $U_{\sigma\sigma'}$ are the different on-site interaction energies which depend on the scattering length between the different species. Both $U_{\sigma\sigma'}$ and τ are functions of the lattice depth. We are interested in a unit-filled lattice in the regime $\tau \ll U_{\sigma\sigma'}$ where the system is deep in the Mott insulating phase [21,22]. In this limit, to zero order in τ the ground state is multidegenerate and corresponds to all possible spin configurations with one atom per site. A finite τ breaks the spin degeneracy. By including virtual particle-hole excitations one can derive an effective Hamiltonian which describes the spin dynamics within the one atom per site subspace [23],

$$\hat{H}_{\text{lat}} = \hat{H}_H + \hat{H}_I = -\bar{\lambda} \sum_{\langle i,j \rangle, \alpha} \hat{\sigma}_i^\alpha \hat{\sigma}_j^\alpha - \bar{\chi} \sum_{\langle i,j \rangle} \hat{\sigma}_i^z \hat{\sigma}_j^z. \quad (37)$$

Here the coefficients are $\bar{\lambda} = \tau^2 / U_{\uparrow\downarrow}$ and $\bar{\chi} = \tau^2 (U_{\uparrow\uparrow}^{-1} + U_{\downarrow\downarrow}^{-1} - 2U_{\uparrow\downarrow}^{-1})$. For simplicity we will now restrict the analysis to one-dimensional systems and assume periodic boundary conditions.

\hat{H}_H is spherically symmetric and in terms of collective spin operators it can be written as

$$\hat{H}_H = -\frac{4\bar{\lambda}}{N} \hat{J}^{(0)2} - \frac{4\bar{\lambda}}{N} \sum_{k=1, \dots, N-1, \alpha} \hat{J}_\alpha^{(k)} \hat{J}_\alpha^{(-k)} \cos\left(\frac{2\pi k}{N}\right). \quad (38)$$

All the $N+1$ fully symmetric states with $J=N/2$ are degenerate and span the ground state of \hat{H}_H . \hat{H}_I is not spherically symmetric but we can also write it in terms of collective operators as

$$\hat{H}_I = -\frac{4\bar{\chi}}{N} \hat{J}_z^{(0)2} - \frac{4\bar{\chi}}{N} \sum_{k=1, \dots, N-1} \hat{J}_z^{(k)} \hat{J}_z^{(-k)} \cos\left(\frac{2\pi k}{N}\right). \quad (39)$$

If the condition $\bar{\lambda} \gg \bar{\chi}$ is satisfied, which can be engineered in this atomic system by means of a Feshbach resonance, the effect of the Ising term can be studied by means of perturbation theory. Assuming that at $t=0$ the initial state is prepared within the $J=N/2$ manifold, a perturbative analysis predicts that for times t such that $\bar{\chi}t < \bar{\lambda}/\bar{\chi}$, \hat{H}_H confines the dynamics to the ground-state manifold and transitions outside it can be neglected. As a consequence, only the projection of \hat{H}_I on it, which corresponds to $\mathcal{P}\hat{H}_I = \chi_e \hat{J}_z^{(0)2} + \frac{\bar{\chi}N}{N-1}$ with $\chi_e \equiv -\frac{4\bar{\chi}}{N-1}$, is effective and H_I acts as a long-range Hamiltonian. Here we used the relation $\mathcal{P}_{k \neq 0}[\hat{J}_z^{(k)} \hat{J}_z^{(-k)}] = -\frac{\hat{J}_z^{(0)2}}{N-1} + \frac{N^2}{4(N-1)}$, with \mathcal{P} the projection into the $J=N/2$ subspace. The nonzero projection of the latter term comes from the fact that

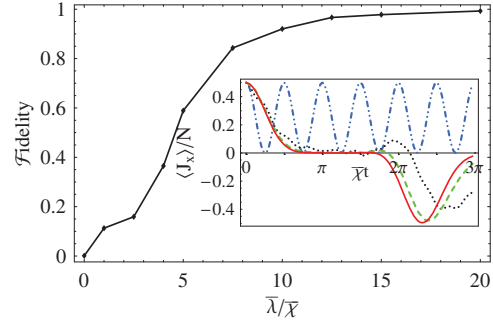


FIG. 8. (Color online) Fidelity to generate a GHZ state vs $\bar{\lambda}/\bar{\chi}$. In the inset we show $\langle \hat{J}_x^{(0)}(t) \rangle$. The x axis there is in units of \hbar . The blue dotted-dashed, dotted black, dashed green, and solid red lines correspond to $\bar{\lambda} = 0, 5, 10, 20$, respectively. The plots are obtained by numerical evolution of Eq. (37) for $N=10$.

the operators $\hat{J}_z^{(k)} \hat{J}_z^{(-k)}$ and $\hat{J}_z^{(0)2}$ are not independent as they satisfy the constraint $\sum_{k=0}^{N-1} \hat{J}_z^{(k)} \hat{J}_z^{(-k)} = N^2/4$.

In Fig. 8 we contrast the dynamical evolution of a system in the presence and absence of \hat{H}_H assuming at time $t=0$ all of the spins are polarized in the x direction. If only the Ising term is present, $\bar{\lambda}=0$, it induces local phase fluctuations that leads to fast oscillations in $\langle \hat{J}_x^{(0)} \rangle = N/2 \cos^2(2\bar{\chi}t)$. On the other hand, as the ratio $\bar{\lambda}/\bar{\chi}$ increases, the isotropic interaction inhibits the fast oscillatory dynamics and instead $\langle \hat{J}_x^{(0)} \rangle$ exhibits slow collapses and revivals. For $\bar{\lambda} \gg \bar{\chi}$ the dynamics exactly resembles the one induced by \hat{H}_c and at $\chi_e t = \pi/2$ the initial coherent state is squeezed into a GHZ state.

B. MPM in lattice systems

\hat{H}_H also provides protection against phase decoherence. However, \hat{H}_H is not as effective as \hat{H}_{prot} because the energy gap between the MPM and the excited states of \hat{H}_H vanishes in the thermodynamic limit as $E_g \rightarrow \bar{\lambda}/N^2$. This is a drawback of the short-range Hamiltonian for the purpose of fully protecting the ground states from long-wavelength excitations. Note, however, that one-dimensional systems are the worst scenario as for higher dimensions the gap vanishes as $N^{-2/d}$ with d the dimensionality of the system. Nevertheless, the many-body interactions can still eliminate short-wavelength excitations since in the large N limit they remain separated by a finite-energy gap, $8\bar{\lambda}$.

We quantify the effectiveness of the MPM to protect the system against \hat{H}_{env} by using time-dependent perturbation theory. For this analysis we restrict to the limit $\bar{\lambda} \gg \bar{\chi}$, where the Ising term can be treated as an effective $\chi_e \hat{J}_z^{(0)2} + \frac{\bar{\chi}N}{N-1}$ Hamiltonian. In this limit a convenient basis to study the quantum dynamics is the collective spin basis. Assuming that at $t=0$ the system lies within the $J=N/2$ manifold, the evolution of the matrix elements $\rho_{MM} \equiv \langle N/2, \tilde{M} | \hat{\rho} | N/2, M \rangle_z$ can be written as

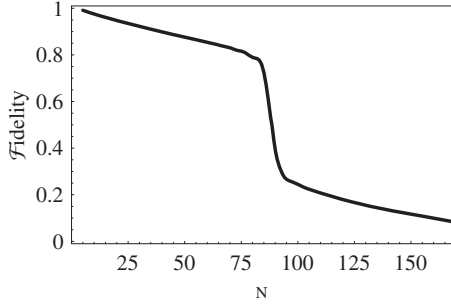


FIG. 9. In the presence of phase decoherence the fidelity of the GHZ state preparation in the lattice is degraded as N grows because in the lattice the gap decreases and the generation time increases with N . In this plot we assumed the limit $\bar{\chi} \ll \bar{\lambda}$, where Eq. (42) holds and used a system with $\omega_c = \bar{\chi}$, $\bar{\lambda} = 100\bar{\chi}$, and $\Gamma = 0.01\bar{\chi}$. At $N=90$, $\Delta E_g = \omega_c$ and it explains the drop of \mathcal{F} for $N > 90$.

$$\rho_{M,\tilde{M}}(t) = \rho_{M,\tilde{M}}(0) e^{it\chi_e(M^2 - \tilde{M}^2)} e^{i(\theta_M - \theta_{\tilde{M}})} e^{-1/2(\gamma_{\text{lat}}^M - \gamma_{\text{lat}}^{\tilde{M}})}, \quad (40)$$

where the random phase, given by Eq. (10), characterizes the dynamics induced by the noise within the MPM and $\gamma_{\text{lat}}^M(t) = \sum_{J \neq N/2, \beta} |\int_0^t d\tau \mathcal{M}_{J,\beta}^M e^{i\tau\omega_{J,\beta}^{\text{lat}}}|^2$, takes into account the depletion of the $J=N/2$ levels due to transition matrix elements with states outside the symmetric manifold, $\mathcal{M}_{J,\beta}^M = \langle \frac{N}{2}, M | \hat{H}_{\text{env}} | J, M, \beta \rangle$. $\omega_{J,\beta}^{\text{lat}}$ are the respective energy splittings. Up to this point the expressions are structurally identical to the ones obtained for long-range interactions. The difference appears in the evaluation of γ_{lat} . In contrast to \hat{H}_{prot} , not only the excitation frequencies $\omega_{J,\beta}^{\text{lat}}$ are not degenerated but also they become smaller as N is increased. As a consequence Eq. (12) is replaced by the following equation for the lattice system:

$$\overline{\gamma_{\text{lat}}^M(t)} \approx \frac{N^2 - 4M^2}{N(N-1)} f \sum_{k=1}^{N-1} \int_0^{\omega_c} d\omega \left(\frac{\sin[t(\omega - \Delta E^k)/2]}{\omega - \Delta E^k} \right)^2 \quad (41)$$

with E^k the excitation energies of the states that belong to the $J=N/2-1$ manifold given by $\Delta E^k = 8\bar{\lambda} \sin^2(\pi k/N)$, with $k = 1, \dots, N-1$ [24]. From Eq. (41) we can estimate the degradation of the fidelity due to phase decoherence as

$$\mathcal{F}(t_o) \geq e^{-\overline{\gamma_{\text{lat}}^0(t_o)}} \frac{1}{\sqrt{1 + \Gamma(t_o)}}. \quad (42)$$

In Fig. 9 we plot \mathcal{F} calculated from Eq. (42) as a function of N . In the lattice the fidelity is degraded as N grows because the gap decreases and the generation time increases with N . Moreover, an abrupt drop of the fidelity occurs at the value of N at which $E_g = \omega_c$.

VI. NOISE AND DECOHERENCE IN LATTICE SYSTEMS

In the preceding section we used the effective Hamiltonian given by Eq. (37) to study the GHZ generation in lattice systems. Here we perform a more detailed analysis of

its validity and estimate the effect of deviations from the ideal situation in an actual experiment. For this analysis we restrict to the limit $\bar{\lambda} \gg \bar{\chi}$ where the Ising term can be treated as an effective $\chi e^{\hat{J}_z^{(0)2}} + \frac{\bar{\chi}N}{N-1}$ Hamiltonian.

A. Particle-hole excitations

Deriving Eq. (37) from the Bose-Hubbard Hamiltonian we only included virtual-particle hole excitation. However, during the time evolution real transitions from singly to doubly occupied states can take place and they degrade the fidelity.

To account for these effects, we write the many-body wave function as $|\Psi(t)\rangle = \sum_n C_n |\psi_n\rangle + \sum_m B_m |\phi_m\rangle$, where $|\psi_n\rangle$ span the Hilbert space with one atom per site and $|\phi_m\rangle$ span the subspace with two particles and one hole adjacent to each other and $N-2$ singly occupied sites. The latter are the states that directly coupled to $|\psi_n\rangle$ through tunneling. Solving the time-dependent Schrödinger equation from the Bose-Hubbard Hamiltonian, using the assumption that $U_{\sigma,\sigma'} \approx U$, and that at time $t=0$ no doubly occupied states are populated, one obtains

$$i\dot{C}_n = \sum_k \langle \psi_n | \hat{H}_{\text{lat}} | \psi_k \rangle (1 - e^{-iUt}) C_k. \quad (43)$$

Here we also assumed that $\{C_n\}$ change at a rate much smaller than U and treated them as constants during the time integration. Equation (43) yields the following lost of fidelity due to real particle hole excitations:

$$\mathcal{F}(t_o) \approx 1 - \frac{4\bar{\chi}}{U} \sin^2(Ut_o/2), \quad (44)$$

remembering that $\chi_e t_o = \pi/2$. As long as $\bar{\chi}/U \ll 1$, we conclude that particle-hole excitations do not significantly affect the GHZ generation.

B. Magnetic confinement

In Eq. (36) we assumed a translationally invariant system. However, in most of the experiments an additional quadratic magnetic confinement is used to collect the atoms. Actually, it is due to this quadratic potential that a unit-filled Mott insulator has been experimentally realized. In its absence it would be difficult to create a unit-filled Mott insulator as in an homogeneous system it only takes place when the number of atoms is exactly equal to the number of lattice sites. A drawback of the magnetic confinement is that it generates always superfluid regions at the edge of the cloud, so only a fraction of the total trapped atoms located at the trap center must be selected as the quantum register. Assuming we work on this unit-filled Mott insulator subspace, here we quantify the effect of the magnetic potential in the GHZ generation in the $\bar{\lambda}/\bar{\chi} \gg 1$ limit.

The magnetic confinement is accounted for by adding a term $W \sum_{j,g} j^2 \hat{n}_{\sigma,j}$ in the Bose-Hubbard Hamiltonian: $W = 1/2m\omega_T^2 a_L^2$ with m the atom mass, ω_T the frequency of the external trapping potential, and a_L the lattice spacing. This term modifies the global coupling constants $\bar{\lambda}$ and $\bar{\chi}$ when

the effective Hamiltonian is derived and makes them site dependent, $\bar{\lambda} \rightarrow \bar{\lambda}_i^W \equiv \tau^2 / \tilde{U}_{i,\uparrow\downarrow}$ and $\bar{\chi} \rightarrow \bar{\chi}_i \equiv \tau^2 (\tilde{U}_{i,\uparrow\uparrow}^{-1} + \tilde{U}_{i,\downarrow\downarrow}^{-1} - 2\tilde{U}_{i,\uparrow\downarrow}^{-1})$. Here $\tilde{U}_{i,\sigma\sigma'} = U_{\sigma\sigma'} / [U_{\sigma\sigma'}^2 - W^2(2i+1)^2]$. Assuming that the gradient of the external potential is weak compared to the on-site interaction energy, as is in general the case for current experiments, the effective Hamiltonian in the presence of the magnetic trap becomes

$$\hat{H}_{\text{lat}}^W = \hat{H}_{\text{lat}} + \hat{H}_1^T, \quad (45)$$

$$\hat{H}_1^T = - \sum_{\langle i,j \rangle} T_i \vec{\sigma}_i \cdot \vec{\sigma}_j, \quad (46)$$

$$T_i = - \frac{\tau^2 W^2 (2i+1)^2}{U^3}. \quad (47)$$

The corrections on the fidelity of the GHZ state introduced by \hat{H}_1^T can be estimated by calculating the effective projection of it on the MPM, $\mathcal{P}\hat{H}_1^T$. As the latter is just proportional to the identity matrix I , $\mathcal{P}\hat{H}_1^T = \sum_i T_i I$, it effects only a global phase and it does not cause any main degradation of the fidelity. Similarly any other perturbation induced by local fluctuations in the magnetic field or the lasers used to generate the lattice become irrelevant thanks to the MPM.

From this analysis we conclude that except from spontaneous emission or heating mechanisms the MPM effectively protects lattice systems against common nonideal situations encountered during their experimental realization. On the other hand, lattice-based GHZ state generation faces the scalability problem due to the fact that the gap decreases and the generation time increases with increasing N .

VII. CONCLUSIONS

In this paper we studied the use of a decoherence-free multilevel manifold for robust preparation of multiparticle GHZ entangled states of trapped ions or cold atoms in an

optical lattice. The MPM is isolated from the rest of the Hilbert space by an energy gap which energetically suppresses any local decoherence processes. We have presented analytical estimates for the fidelity of the GHZ preparation.

In trapped ions we demonstrated that the fidelity can be significantly better than the one achievable without any gap protection and therefore that our scheme is in the position to improve the spectroscopy resolution in current Ramsey spectroscopy experiments.

We also showed that cold atoms in optical lattices interacting via short-range interactions can be utilized to engineer long-range interactions which in turn can be used for generating many-body entanglement. We calculated the effects of nonideal conditions and concluded that the main restriction in these systems is the scalability as the MPM protection degrades with increasing N .

The scalability certainly limits the use of lattice systems for massive entanglement generation, however it is not a problem for recent quasi-one-dimensional experiments [25] where an array of 1D tubes with an average of 18 atoms per tube has been realized. In such systems therefore it should be possible to create few-particle collective entangled states using our scheme and to perform proof-of-principle experiments demonstrating the improvement of spectroscopic sensitivity.

We emphasize that, even though we have limited the discussion to ensembles of spin $S=1/2$ particles, the MPM ideas can be straightforwardly generalized to systems composed of higher spin atoms. Besides entanglement generation, the MPM might have also important applications for the implementation of good storage memories using, for example, nuclear spin ensembles in solid state [26] or photons [27].

ACKNOWLEDGMENTS

This work was supported by ITAMP, NSF (Career Program), USAFOSR, ONR MURI, and the David and Lucille Packard Foundation.

-
- [1] M. Nielsen and I. Chuang, *Quantum Computation and Quantum Communication* (Cambridge University Press, Cambridge, 2000).
- [2] J. Preskill, *J. Mod. Opt.* **47**, 127 (2000).
- [3] D. Leibfried *et al.*, *Science* **304**, 1476 (2004).
- [4] D. Leibfried *et al.*, *Nature (London)* **438**, 639 (2005).
- [5] A. M. Rey, L. Liang, M. Fleischhauer, E. Demler, and M. Lukin, e-print arXiv: cond-mat/0703108.
- [6] D. M. Greenberger, M. A. Horne, A. Shimony, and A. Zeilinger, *Am. J. Phys.* **58**, 1131 (1990).
- [7] K. Mølmer and A. Sørensen, *Phys. Rev. Lett.* **82**, 1835 (1999).
- [8] A. Sørensen and K. Mølmer, *Phys. Rev. A* **62**, 022311 (2000).
- [9] G. J. Milburn, S. Schneider, and D. F. V. James, *Fortschr. Phys.* **48**, 801 (2000).
- [10] F. T. Arecchi, E. Courtens, R. Gilmore, and H. Thomas, *Phys. Rev. A* **6**, 2211 (1972).
- [11] J. J. Bollinger, W. M. Itano, D. J. Wineland, and D. J. Heinzen, *Phys. Rev. A* **54**, R4649 (1996).
- [12] S. F. Huelga, C. Macchiavello, T. Pellizzari, A. K. Ekert, M. B. Plenio, and J. I. Cirac, *Phys. Rev. Lett.* **79**, 3865 (1997).
- [13] A. Papoulis, *Probability, Random Variables, and Stochastic Processes* (McGraw-Hill, New York, 1965).
- [14] R. G. Unanyan and M. Fleischhauer, *Phys. Rev. Lett.* **90**, 133601 (2003).
- [15] D. F. V. James, *Fortschr. Phys.* **48**, 823 (2000).
- [16] C. Langer *et al.*, *Phys. Rev. Lett.* **95**, 060502 (2005).
- [17] G. Morigi and S. Fishman, *Phys. Rev. Lett.* **93**, 170602 (2004).
- [18] R. Ozeri *et al.*, *Phys. Rev. Lett.* **95**, 030403 (2005).
- [19] C. W. Gardiner, *Quantum noise* (Springer, Berlin, 1991).
- [20] D. Jaksch, C. Bruder, J. I. Cirac, C. W. Gardiner, and P. Zoller,

- Phys. Rev. Lett. **81**, 3108 (1998).
- [21] M. P. A. Fisher, P. B. Weichman, G. Grinstein, and D. S. Fisher, Phys. Rev. B **40**, 546 (1989).
- [22] M. Greiner *et al.*, Nature (London) **415**, 39 (2002).
- [23] L.-M. Duan, E. Demler, and M. D. Lukin, Phys. Rev. Lett. **91**, 090402 (2003).
- [24] B. Sutherland, *Beautiful Models* (World Scientific, Singapore, 2004).
- [25] B. Paredes *et al.*, Nature (London) **429**, 277 (2004).
- [26] A. C. Johnson *et al.*, Nature (London) **435**, 925 (2005).
- [27] C. Mewes and M. Fleischhauer, Phys. Rev. A **72**, 022327 (2005).